

# Novel small synthetic HIV-1 V3 crown variants: CCR5 targeting ligands

Received 3 January 2022; accepted 2 June 2022; published online 16 June 2022

Anju Krishnan Anitha<sup>1,2</sup>,  
Pratibha Narayanan<sup>1,2</sup>,  
Neethu Ajayakumar<sup>1,2</sup>,  
Krishnankutty Chandrika Sivakumar<sup>1</sup> and  
Kesavakurup Santhosh Kumar<sup>1,†</sup>

<sup>1</sup>Chemical Biology Laboratory, Pathogen Biology Research Program, Rajiv Gandhi Centre for Biotechnology, Thiruvananthapuram 695014, India; and <sup>2</sup>University of Kerala, Thiruvananthapuram, Kerala, 695014, India

<sup>†</sup>Kesavakurup Santhosh Kumar, Chemical Biology Laboratory, Pathogen Biology Research Program, Rajiv Gandhi Centre for Biotechnology, Thiruvananthapuram 695014, India. Tel.: +91471 2529518, email: kskumar@rgcb.res.in

The CC chemokine receptor 5 (CCR5) antagonism represents a promising pharmacological strategy for therapeutic intervention as it plays a significant role in reducing the severity and progression of a wide range of pathological conditions. Here we designed and generated peptide ligands targeting the chemokine receptor, CCR5, that were derived from the critical interaction sites of the V3 crown domain of envelope protein glycoprotein gp120 (TRKSIHIGPGRAFYYTGEI) of HIV-1 using computational biology approach and the peptide sequence corresponding to this region was taken as the template peptide, designated as TMP-1. The peptide variants were synthesized by employing Fmoc chemistry using polymer support and were labelled with rhodamine B to study their interaction with the CCR5

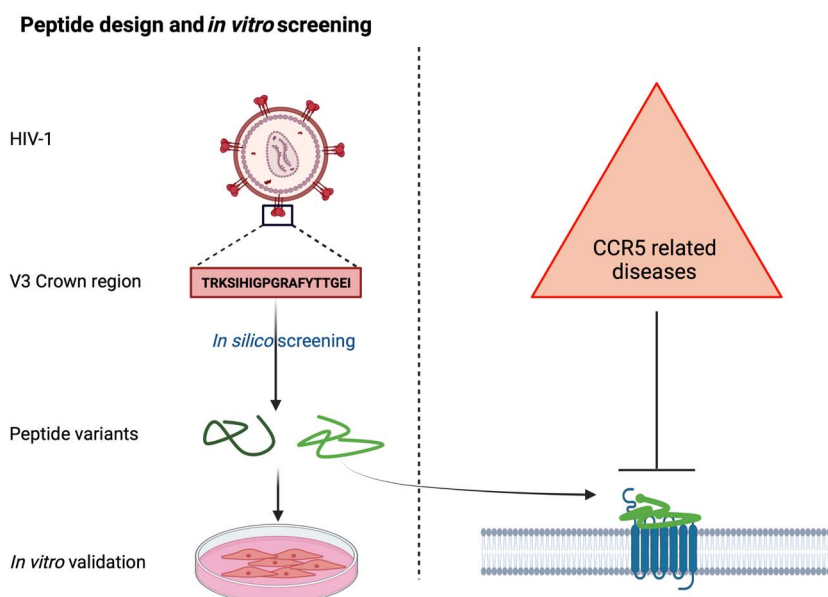
receptor expressed on various cells. TMP-1 and TMP-2 were selected as the high-affinity ligands from *in vitro* receptor-binding assays. Specific receptor-binding experiments in activated peripheral blood mononuclear cells and HOS.CCR5 cells indicated that TMP-1 and TMP-2 had significant CCR5 specificity. Further, the functional analysis of TMP peptides using chemotactic migration assay showed that both peptides did not mediate the migration of responsive cells. Thus, template TMP-1 and TMP-2 represent promising CCR5 targeting peptide candidates.

**Keywords:** V3 crown; RANTES; gp120; CCR5 antagonism; CCR5.

## Introduction

CC chemokine receptor 5 (CCR5), which is a member of the  $\beta$  chemokine receptor family, is mainly expressed on various immune cells, neurons, astrocytes, microglia, vascular smooth muscle and fibroblasts (1, 2). It is a key player in mediating the migration of cells during the immune response. On the contrary, it acts as a doorway for the development of various pathological conditions, including autoimmune diseases, allergic diseases, cancers and bacterial infections as well as in several viral infections caused by HIV-1, Zika virus, Epstein Barr virus, Rhinovirus, Rocio virus and Hepatitis B virus (3–7).

## Graphical Abstract



CCR5 blockade represents a potential therapeutic approach to combat CCR5-related diseases. It is achieved either by employing gene-editing strategies to disable the cell surface expression of CCR5 or by CCR5 antagonism using various molecular entities. It was reported as an effective strategy to treat several cognitive defects, multiple sclerosis, neuroinflammation and various cancers including breast cancer, ovarian cancer, prostate cancer, colorectal cancer, melanoma, multiple myeloma and gastric cancer (8–13). CCR5 $\Delta$ 32 mutation, which prevents the cell surface expression of CCR5, was reported to provide resistance against HIV-1 infection, rheumatoid arthritis and coronary artery disease (14–16). Reports suggest that CCR5 antagonism is effective against Crimean-Congo hemorrhagic fever, vaccinia virus infection, HIV infection and *Staphylococcus aureus* pathogenesis (17–20). CCR5 targeting gained momentum again during the COVID-19 pandemic situation, with the identification of its involvement in the clinical progression of SARS-CoV-2 infection. CCR5 antagonism has also been reported as a potential treatment modality to combat corona infection, as CCR5 antagonists were found to be effective in treating the immune dysregulation caused by SARS-CoV-2 infection leading to the cytokine storm (21–23). The involvement of CCR5 in the development of various bacterial, parasitic, fungal and viral infections and the associated immune dysregulation accelerated the efforts to develop CCR5 inhibitors as anti-infectives.

CCR5 targeting molecular entities mainly come under four categories: chemokine analogues, small molecule inhibitors, peptide-based inhibitors and monoclonal antibodies. Chemokine analogues represent the first generation CCR5 antagonists, as the endogenous chemokines serve as an excellent template for the generation of chemokine-based CCR5 antagonists. RANTES (regulated upon activation, normal T cell expressed and presumably secreted) is the extensively modified endogenous chemokine for developing chemokine analogues targeting CCR5 and few RANTES variants, such as AOP-RANTES and PSC-RANTES, showed excellent HIV-1 inhibitory activity (24, 25). Peptide T is a peptide-based CCR5 antagonist derived from the V2 region of gp120. It binds competitively to the CCR5 and blocks the interaction between gp120/CD4 and CCR5 (26). Maraviroc, a small molecule CCR5 inhibitor developed by Pfizer, is the first Food and Drug Administration (FDA)-approved CCR5 antagonist for the treatment of naive and treatment-experienced HIV patients (27). In addition to this, the efficacy of maraviroc against several pathological conditions, including COVID-19, is being evaluated in clinical trials (28–32). Cenicriviroc is another small molecule CCR5 antagonist, which binds to a domain other than the extracellular loop 2 and the N terminus of CCR5 and induces a conformational change in the CCR5. It showed promising effects against HIV-1 infection, liver fibrosis and fatty liver (33–35). It is also under clinical trials against HIV-1 and COVID-19 (36, 37). Leronlimab (PRO-140) is a humanized monoclonal antibody that recognizes N-terminal and extracellular loop 2 of CCR5, which showed excellent effectiveness against HIV-1 infection, is currently retasked for triple-negative breast cancer, COVID-19, Graft-versus-host disease (37–41). There are a growing number of CCR5 antagonists in various phases of pre-clinical and

clinical trials for the treatment of CCR5-related diseases (37).

As important as druggable target identification, the selection of a candidate molecule that can be used as the template to design CCR5 inhibitor is also critical in achieving effective receptor blockade. Since the CCR5 in complex with HIV-1 gp120 is well studied, the exploitation of such interaction interface holds great possibility to design potent CCR5 inhibitors. The crucial component of HIV-1 envelope protein involved in the initial interaction of both viral and host cell membrane is the envelope glycoprotein subunit: gp120. The gp120 subunit is composed of five relatively conserved (C1–C5) and five variable (V1–V5) domains (42, 43). The amino acid residues in the third variable region (V3) of gp120 serve as the major determinants of coreceptor selectivity, cellular tropism (44–55). The V3 region, which consists of approximately 35 amino acid residues, shows a high degree of sequence diversity among various isolates and is one of the major immunogenic sites in the virus (56–58). Topologically, the V3 domain is divided into three distinct regions: the base, the stem and the tip or crown.

In this study, we selected the V3 crown region and the few residues flanking on both sides of the V3 crown to generate CCR5 targeting ligands, as the residues in the crown region have been identified as the major determinants for coreceptor usage (59). The peptide derived from this region was termed TMP-1 and the possible interactions between the TMP-1 and CCR5 were exploited to generate high-affinity CCR5-binding ligands. The variants were designed by employing a systemic mutation approach, in which the certain amino acid residues of the TMP-1 were replaced with other residues based on the intermolecular interaction free energy of TMP-1:CCR5 complex and the available literature. The computationally derived complete structure of TMPs in complex with CCR5 receptor structure showed that the peptides interacted with CCR5 residues in the N-terminus, extracellular loop 1, 2 and 3 and transmembrane helices 1, 2, 3, 6 and 7. The *in vitro* receptor-binding experiments using rhodamine B-labelled TMP-1 and variants conducted on CCR5 expressing cells showed that TMP-1 and TMP-2 displayed significantly higher binding ability than TMP-3 and TMP-4. The specificity of TMP-1 and TMP-2 towards CCR5 highlights their feasibility as efficacious CCR5 targeting candidate molecules.

## Materials and Methods

### Materials

RANTES Human Recombinant, Anti-Human CD195 (T21/8), Fluorescein Goat anti-mouse IgG(H + L), Ficol-Paque Plus, Hoechst stain, MTT (3-(4,5-dimethylthiazol-2-yl)-2,5-diphenyl tetrazolium bromide) dye, rhodamine B, CLEAR Resin, Rink amide linker and Fmoc protected amino acids, phytohaemagglutinin P (PHA-P).

Human osteosarcoma cells (HOS.CCR5) stably expressing CCR5 receptors were obtained from NIH AIDS Reagent Program, Division of AIDS, and were treated as per the protocol mentioned by the NIH AIDS Reagent Program for culturing and maintaining. The cells were cultured in DMEM and were supplemented with 10% heat-inactivated foetal bovine serum and 1% Penicillin

Streptomycin (Pen Strep) (Gibco, Life Technologies, Waltham, Massachusetts, USA) at 37°C containing 5% CO<sub>2</sub>. THP -1 monocyte cells were obtained from the National Centre for Cell Sciences (Pune, India). The cells were cultured in RPMI 1640 (Gibco) and were supplemented with 10% heat-inactivated foetal bovine serum and 1% Pen Strep. Peripheral blood mononuclear cells (PBMCs) were freshly isolated from whole blood of healthy donors according to the standard protocol described using Ficoll-Paque Plus (GE Health care, Chicago, Illinois, USA) (Institutional Human ethical committee No. IHEC/1/2013/09) (60). The freshly isolated PBMCs were activated with phytohemagglutinin (PHA-P) (5 µg/ml) (Sigma-Aldrich, Missouri, USA) in DMEM with 10% FBS for 48–72 hours prior to the experiment at 37°C.

### Methods

**Selection of template** The V3 crown region of gp120, along with the flanking residues from both N and C-terminal region of the V3 stem was selected as the reference peptide for generating the CCR5 targeting ligands, as the CCR5 utilization of the gp120 envelope protein is primarily mediated by the residues in the V3 crown region of V3 loop (59, 61). The V3 loop is composed of approximately 35 residues, in which residues 1 and 35 are connected through a disulphide bridge. It possesses a net-positive charge, which can vary from +2 to +10 (47, 62).

**Binding-free energy analysis of template peptide and designing of CCR5 targeting variants** The primary sequence of the template was retrieved from the solution NMR structure of the V3 loop of the envelope protein gp120 from RCSB Protein Data Bank with PDB ID: 1CE4. The X-ray crystallography structure of the Maraviroc bound CCR5 was obtained from RCSB Protein Data Bank with PDB ID: 4MBS (63, 64). The alignment of V3 loop residues obtained from the PDB data is represented in the Fig. 1A. The binding-free energy and the critical interacting residues of the selected V3 crown region with the CCR5 receptor structure were analysed by molecular dynamics simulations using Gromacs 4.5.5 in a membrane-mimicking environment (65). The binding-free energy of the peptide residues was estimated using the *g\_nmpbsa* module (66) by taking snapshots at every 10 ps from the 20 ns production run and the whole process was repeated until sufficient good scoring variants were received.

The residues in the template peptide with favourable binding energy and those reported as conserved were preserved. A systemic mutation approach was adopted to substitute residues with unfavourable binding energy with other amino acids in order to generate novel peptide variants. The variants were then modelled using Modeller 9.17. The modelled variants were then subjected to ZDock to predict their interaction with the receptor. ZDOCK uses a grid-based representation of two proteins and a 3-dimensional fast Fourier transform to explore the rigid-body search space of docking positions (67). The variants with better binding score than the TMP-1 were selected and were further subjected to molecular dynamics simulations using Gromacs 4.5.5 in a membrane-mimicking environment (65).

**Chemical synthesis of CCR5 targeting peptide variants** The peptide ligands were synthesized on Cross-Linked Ethoxylate Acrylate resins (CLEAR resin) using Fmoc protected amino acids (Peptides International, Louisville, USA). On-resin fluorochrome (rhodamine B) labelling of peptides was also done. Following synthesis, the peptides were cleaved from the resin by treating with the cleavage cocktail comprising of TFA (95% v/v), thioanisole (2.5% v/v) and water (2.5% v/v) at room temperature for 3 hours with gentle intermittent stirring. The filtrate was collected, concentrated under vacuum, precipitated by ice-cold diethyl ether and recovered by centrifugation. The recovered peptide ligands were purified by RP-HPLC (Shimadzu) using Phenomenex Luna5u C18 analytical column (250 × 4.6 mm). Chromatographic separation was employed using a gradient mobile phase with a flow rate of 1 ml/min and the column temperature was kept up to 40°C. The detection was accomplished at 214, 510 and 540 nm. MALDI-TOF-MS analysis was performed using Bruker Daltonics Ultraflex MALDI TOF/TOF mass spectrometer to confirm the molecular mass of the peptide ligands.

**Evaluation of CCR5 expression** The expression of CCR5 on the HOS.CCR5, PBMC and THP-1 monocyte cell line was validated using anti CCR5 monoclonal antibody (T21/8) (eBioscience, Thermo Fisher Scientific, Waltham, Massachusetts, USA). Cells were resuspended in 1X PBS to a concentration of 5 × 10<sup>5</sup> cells per reaction tube. The cells were blocked with 1% BSA in PBS and then incubated with 15 µg/ml anti-CCR5 monoclonal antibody for 3 hours at 4°C, followed by incubation with FITC-labelled secondary antibody (Invitrogen, Thermo Fisher Scientific, Waltham, Massachusetts, USA) for 1 hour in dark at 4°C. The fluorescence associated with the cells per sample was analysed using Flow cytometry (BD FACS Aria III).

**Screening for the binding ability of TMP variants to CCR5** FACS-based ligand binding assay was done to determine the binding ability of variants. A single concentration of rhodamine-labelled variants (20 µM) was treated to the HOS.CCR5 cells and kept for 60 minutes at 4°C. Cells were then centrifuged at 2000 rpm for 3 minutes; the supernatant was then discarded and washed with 1X PBS twice. The cells were resuspended in DMEM medium, and the fluorescence was analysed by flow cytometry.

**Evaluation of ligand binding by confocal microscopy** HOS.CCR5 cells were cultured on a coverslip at a density of 1 × 10<sup>4</sup> cells/well overnight. The media was removed and washed twice with 1X PBS before the treatment of samples. A single concentration (20 µM) of rhodamine-labelled variants was added to the coverslip and incubated for 60 minutes at 4°C. The unbound variants were washed using 1X PBS, then the samples were fixed in 4% formaldehyde and all samples were incubated with 10 µg/ml Hoechst to stain the nuclei of the cells. Finally, the coverslips were mounted and imaging was performed using confocal microscopy (Leica SP8 WLL).

**Analysis of CCR5 binding affinity of variants** TMP-1 and TMP-2 at different concentration were treated in cells expressing varying levels of CCR5 (HOS.CCR5, THP-1 and PBMCs) and incubated for 1 hour at 4°C. The cells were then

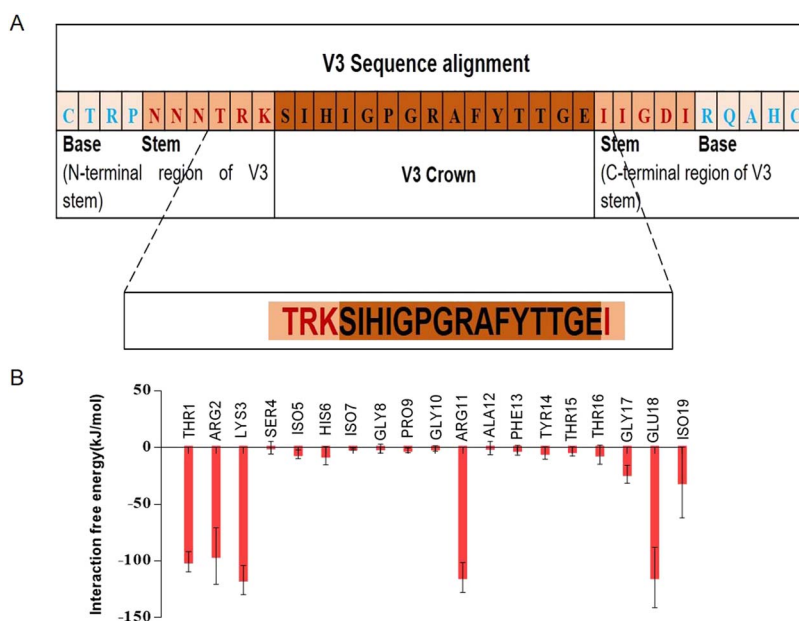


**Fig. 1. (A) Representative diagram showing the alignment of the V3 domain sequence obtained from PDB accession code 1CE4 and the amino acid sequence of the selected region of V3 crown for designing variants.** The peptide derived from this region (TRKSIHIGPGRAFYTTGEI) was named TMP-1. **(B)** Interaction free energies of individual TMP-1 residues in complex with CCR5 (intermolecular interaction free energies (y-axis) and TMP-1 residues (x-axis)).

centrifuged at 1500 rpm for 3 minutes and unbound ligands were removed by washing three times with 1X PBS buffer and were resuspended in 500  $\mu$ l DMEM for flow cytometry analysis.

**Effect of TMP binding on CCR5 specific antibody binding** The PBMCs cultured in the presence of PHA were harvested and centrifuged at  $400 \times g$  and treated with 20  $\mu$ M of TMP-1 and TMP-2. The treated cells were incubated at 4°C for 1 hour and then washed three times with 1X PBS to remove unbound ligands. Following this, 15  $\mu$ g/ml of monoclonal antibody (T21/8) against CCR5 was added and incubated at 4°C for 3 hours and, finally, the cells were incubated for 1 hour with a secondary antibody conjugated with FITC at dark. The control wells were treated with media alone. The cells that were treated only with antibody served as the comparative sample. The cells were then washed with PBS thrice to remove the unbound secondary antibody and the samples were analysed by flow cytometry.

**Specific binding of TMP variants** A competitive binding strategy was adopted to determine the specificity of variants using excess endogenous ligand of CCR5 receptor, RANTES (Sigma-Aldrich);  $5 \times 10^5$  HOS.CCR5 cells were treated with either excess RANTES and single concentration (20  $\mu$ M) of rhodamine-labelled TMP variants or TMP variants alone. Following the incubation for 60 minutes at 4°C, the cells were washed thrice using 1X PBS to remove the unbound peptides. The cells treated with the variants alone served as the comparative control and the untreated cells served as the control.

**Chemotactic migration assay** Two strategies were adopted to examine the chemotactic activity of TMP variants towards HOS.CCR5 cells. Using Transwell chambers (Corning,

New York, USA), the responsive cell migration towards the variants was quantified. The cells were treated with serum-free medium for 5 hours prior to the treatment of variants. Different concentration of the TMP variants (0.1, 1.0, 10, 100  $\mu$ M) were added to the lower wells of the chamber, and cells in FBS-free medium were added to the upper chamber. The upper and lower chambers were separated by a filter of pore size of 8  $\mu$ M. The whole chamber was incubated at 37°C for 4 hours. The filter was then removed and migrated cells were fixed and stained by crystal violet and counted in three microscopic fields. Two inserts were used for each treatment, in which the control group was treated with media alone and RANTES (10 nM)-treated cells served as the positive control.

Agarose spot assay was done to confirm the variant-mediated chemotaxis of responsive cells (68). A total of 0.5% agarose in PBS was heated on a hot plate and stirred till complete dissolution. After complete melting, it was cooled to 40°C. The variants at the concentration of 0.1, 1.0, 10 and, 100  $\mu$ M were prepared in 0.5% agarose in PBS. The spots of peptide-containing agarose (20  $\mu$ l) were placed in each well and were allowed to solidify at 4°C for 5 minutes. The spots containing PBS alone and RANTES (10 nM) served as the control and positive control, respectively. A total of  $5 \times 10^5$  cells along with FBS free media were added to each well and incubated for 4 hours in a CO<sub>2</sub> incubator. The media along with cells were replaced with fresh media and imaging was performed.

**CCR5 internalization assay** The down-modulation of cell surface CCR5 was done as per previously published protocols (69–71). The activated PBMCs were seeded in six-well plates and incubated overnight at 37°C. The following day, the media was replaced with fresh FBS-free media and incubated for 3 hours prior to the experiment. The cells



were treated with different concentration of variants (0.1, 1.0, 10, 100  $\mu\text{M}$ ) and RANTES (10 nM) and incubated for 60 minutes at 37 °C, transferred to 4°C and kept for 5 minutes, and washed with ice-cold acid stripping buffer. The unbound CCR5 was then stained by anti-CCR5 monoclonal antibody for 3 hours at °C and then with the secondary antibody for 1 hour at dark. The cells treated with RANTES served as positive control. The fluorescence was quantified by flow cytometry analysis.

**In vitro toxicity studies of variants** The cytotoxic effect of variants against HOS.CCR5 cells and isolated PBMCs was evaluated by MTT assay (72). HOS.CCR5 cells ( $1 \times 10^5$ ) and PBMCs ( $1 \times 10^4$ ) were seeded in each well of 96-well plates and kept overnight in DMEM medium containing 10% FBS. Cells were then incubated in the presence of various concentration of variants over 48 hours. Cells treated with 1% TritonX100 were used as the positive control. The cells were then treated with 100  $\mu\text{L}$  of MTT solution (5 mg/ml) and incubated for 4 hours at 37°C. The insoluble formazan product was solubilized by the addition of DMSO to each well and the optical density was measured at 570 nm after 10 minutes using a microplate reader (Biorad).

Hemolytic activity of variants was determined by treating various concentration of peptides in suspensions of human RBC. A total of 5 ml of human blood was drawn directly into EDTA coated tubes. The blood was centrifuged at  $800 \times g$  for 10 minutes at 4°C; the levels of haematocrit and plasma were marked on the tube; and the plasma layer was aspirated. A total of 150 mM NaCl was added up to the mark and mixed by inversion. The whole content was then centrifuged at  $500 \times g$  and the supernatant was aspirated. 1X PBS was added up to the mark and spun at  $500 \times g$  for 5 minutes and washed twice using PBS. The optical density of the blood was adjusted to 1.2 at  $\lambda 600$  using 1X PBS. Red blood cells were then incubated at room temperature for 30–45 minutes in 1% Triton X-100 (positive control), in PBS (blank), and with TMP variants. The treated samples were centrifuged at  $800 \times g$  for 5 minutes, the supernatant was separated and the absorbance was measured at 540 nm. The percentage hemolysis of treated samples was analysed by determining the absorbance value compared to that of positive control.

**Statistical Analysis** Data are expressed as mean  $\pm$  S.E. of two independent experiments. The statistical significance was performed by two-tailed unpaired Student's *t*-test or one-way analysis of variance (ANOVA) followed by Dunnett's multiple comparison test. The analysis was done using GraphPad Prism 6 software. The statistically significant results are represented in the graph with stars (\*, \*\*).

## Results

### Selection of template and preparation of the receptor

The region between the N and C-terminal end located within 8–26 residues (TRKSIHIGPGRAFYTTEI) of the V3 region (303–321 residues of gp120), comprising primarily of V3 crown of HIV-1 gp120 was selected as the template for designing peptide variants targeting CCR5

(Fig. 1A) (59). The template peptide is designated as TMP-1 throughout the study. The direct interaction of V3 crown-derived peptides to the CCR5 receptor was examined by *in silico* approach. The N-terminal region of CCR5, which is critical for HIV-1 gp120 binding, ligand binding and coreceptor functioning, was not solved in the crystal structure and was modelled using Modeller 9.17 (PDB ID: 4MBS) (73–75).

### Intermolecular interaction free energy of TMP-1 in complex with CCR5

The interaction of 19-mer template peptide sequence 'TRKSIHIGPGRAFYTTEI' (TMP-1) with CCR5 was performed using ZDock and molecular dynamics simulations. The preliminary docking of the TMP-1 with the CCR5 receptor structure (PDB ID: 4MBS) was done to obtain the TMP-1:CCR5 complex structure, which was further subjected for molecular dynamic simulation studies in a membrane-mimicking environment to obtain the free energy of binding. The intermolecular interaction free energy analysis of TMP-1 in complex with CCR5 validated the contribution of each residue in TMP-1 for their interaction with CCR5. The residues Thr1, Arg2, Lys3 (Thr303, Arg304, Lys305), Arg11, Gly17, Asp18 and Ile19 (Arg313, Gly319, Asp320, Ile321) showed higher interaction free energy (Fig. 1B). Residues Arg2, Lys3 and Arg11 have already been reported to be critical in CCR5 binding, and their replacement has been shown to reduce the CCR5 utilization and binding (76, 77). The conserved GPG motif -Gly8, Pro9 and Gly10 (Gly310–Pro311–Gly312) located in the V3 crown region did not show significant influence on binding affinity in terms of the binding score.

### Designing and chemical synthesis of TMP variants

TMP variants were designed primarily based on the available literature and the obtained intermolecular interaction free energies of individual amino acid residues of TMP-1:CCR5 complex. The residues with the highest negative binding energy score and those residues that were reported to have a key role in CCR5 binding and specificity were retained in most of the variants. Thus, three variants (TMP-2, TMP-3, TMP-4) were generated and were subjected to ZDock and molecular dynamic simulation analysis in a membrane-mimicking environment (78). Interestingly, all the variants showed significantly higher dock score and binding energy scores than the TMP-1 (Table. 1). Residues Arg2 and Lys3, which were already reported to be critical in CCR5 binding, were retained in all the variants. A conservative replacement strategy was adopted for the arginine residue at the 11th position (R11), which was experimentally shown as a key residue in CCR5 utilization (76, 77). The residue Arg11 of TMP-2 and TMP-3 was replaced by Lys11 (R11K). The more conserved GPG motif -Gly8, Pro9 and Gly10 (Gly310–Pro311–Gly312) located in the V3 crown region, which was reported to have a significant role in offering the conformational flexibility to the V3 loop, was also retained in all the variants (79–81). All the designed variants were found to be interacting with the same region of the CCR5 (Fig. 2; Supplementary Fig. 1). The computationally derived complete structure of TMPs in complex with CCR5 receptor structure showed that the peptides

**Table 1. Total binding energy values of the TMP-1 and variants obtained by ZDock and molecular dynamic simulation**

Variants	Sequence	ZDock score (cal/mol)	Binding score (kJ/mol)
TMP-1	TRKSIHIGPGRAFYYTGEI	-1435.4	-509.8
TMP-2	TRKRIHLGPGKAFYTTGDV	-441801.4	-657.2
TMP-3	TRKSISFGPGKAYTTGDI	-406940.8	-540.69
TMP-4	TRKSVHVGPGRAFYYTGEA	-94372.3	-530.9

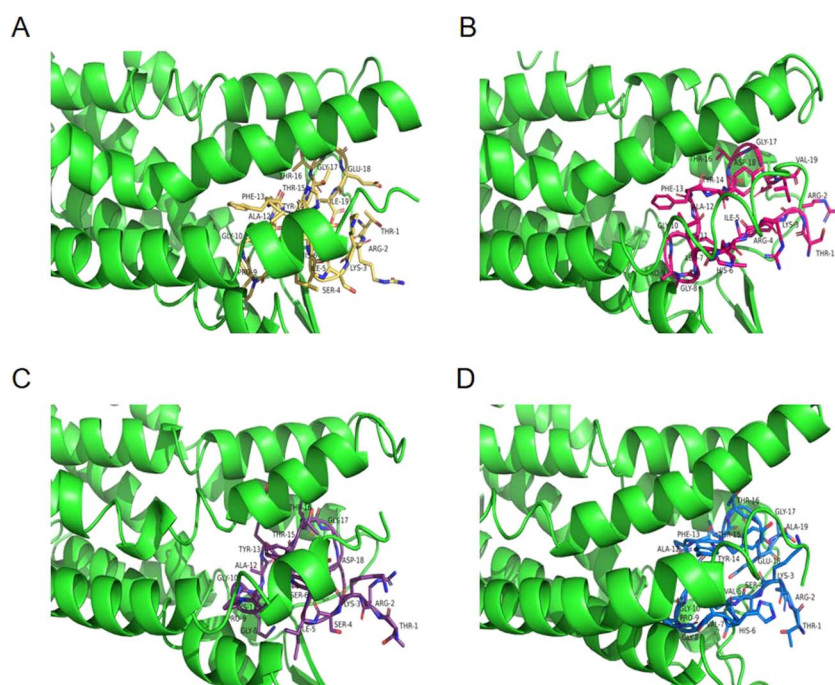


**Fig. 2. Interaction of TMP with CCR5.** The structure of (A) CCR5:TMP-1, (B) CCR5:TMP-2, (C) CCR5:TMP-3 and (D) CCR5:TMP-4 generated by molecular dynamic simulation. The CCR5 receptor structure is represented in green, and the TMP variants are represented in yellow, pink, purple and blue.

interacted with CCR5 residues in the N-terminal region, extracellular loop (ECL1), ECL2, ECL3, transmembrane helical region 1 (TM 1), TM 2, TM 3, TM 6 and TM 7, through van der Waals,  $\pi$ - $\pi$  and hydrogen bond interactions. The residues in the TMP-1 were predominantly involved in the interaction with the residues in N-terminal region, ECL2 and TM 2 of CCR5. The residues in the TMP-2 were found to predominantly interacting with the CCR5 residues in N-terminal region, ECL1, ECL2 and TM 2, whereas TMP-4 residues were mainly interacting with CCR5 N-terminal, ECL1 and TM7 and, finally, the residues in the TMP-3 were primarily involved with residues in the ECL2, TM6 and TM 7 (Supplementary Tables I–IV).

The unlabelled and rhodamine B-labelled TMP-1 and variants were chemically synthesized by Fmoc-solid phase peptide synthesis. The unlabelled peptide variants were purified by RP-HPLC under the detection wavelength of 214 nm. It is evident from the chromatogram of the variants that the retention time of all the variants followed a similar pattern, which could be due to the sequence homology of the variants. The labelled TMP variants were also purified with the detection wavelength of 510 and 540 nm. The molecular weight of both the unlabelled and labelled variants was confirmed by MALDI-TOF-mass spectroscopy (Supplementary Table. V; Supplementary Fig. 2-9).

#### Evaluation of CCR5 expression

HOS.CCR5 cells, THP-1 monocyte cells and human PBMCs were evaluated for the CCR5 cell surface expression using T21/8 monoclonal antibody, mapped to the N-terminal domain of CCR5. It has already been reported that CCR5 expression in PBMCs is more in the case of HIV-1-infected individuals compared with that of normal individuals (82). The majority of the CCR5 in the PBMCs are expressed mainly by the monocyte component (80%), whereas the lymphocyte component expresses ~50% CCR5 (83). The percentage of CCR5 expression in PBMC was obtained as  $75 \pm 2.4\%$ . The monocytes predominantly express CCR5, and it was reported that the THP-1 monocytes after Phorbol myristate acetate (PMA) treatment express ~96.9% CCR5 (84). Our immunostaining results also showed a similar pattern of CCR5 expression in THP-1 cells. The staining of anti-CCR5 antibody with THP-1 monocyte cells after 72 hours of PMA treatment showed  $95 \pm 0.3\%$  FITC positive cells. HOS.CCR5 cells showed  $99 \pm 5\%$  FITC positive cells (Supplementary Fig. 10A, B).

#### Binding ability of TMP variants

The CCR5-binding ability of TMP-1 and the designed variants was evaluated by flow cytometry analysis. The

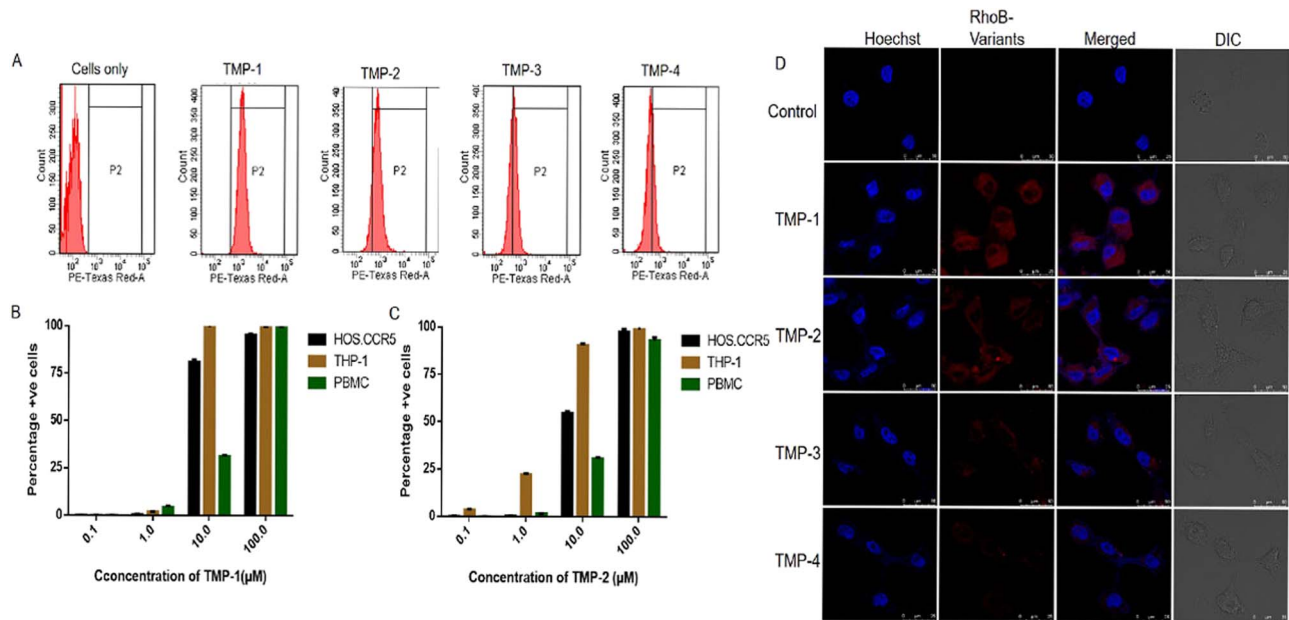


**Fig. 3. The binding ability of rhodamine-labelled TMP variants with CCR5 analysed using flow cytometry and confocal microscopy.** (A) The histogram showing the rhodamine-positive cells in control: TMP-1, TMP-2, TMP-3, TMP-4. TMP-1 and TMP-2 showed significant binding with CCR5, whereas the cell population treated with TMP-3 and TMP-4 did not show binding activity. The quantitative overview of binding of (B) TMP-1 and (C) TMP-2 with CCR5 expressing cells. The binding of varying concentration of TMP variants to HOS.CCR5, THP-1 and PBMCs in terms of percent rhodamine B-positive population was obtained by flow cytometry analysis. TMP-1 and TMP-2 showed a concentration-dependent binding in all three cells. Data are expressed as mean  $\pm$  S.D. of two independent experiments. (D) Confocal microscopy images of TMP variants treated HOS.CCR5 cells with nuclei stained with Hoechst and rhodamine B-tagged TMP-1, TMP-2, TMP-3 and TMP-4 were observed.

HOS.CCR5 cells were treated with single concentration (20  $\mu$ M) of rhodamine-labelled peptides (TMP-1, TMP-2, TMP-3, TMP-4) and incubated for 60 minutes at 4°C. The cells that were not treated with peptides were taken as control. The cells treated with TMP-1 and TMP-2 showed significant rhodamine B fluorescence compared with that of cells treated with TMP-3 and TMP-4 (Fig. 3A). The binding ability in the terms of rhodamine-positive cells showed that the peptide derived from the V3 region of gp120 (TMP-1) had the highest binding activity among the variants followed by TMP-2, TMP-3 and TMP-4. Confocal microscopic studies of rhodamine B-labelled peptides binding to CCR5 confirmed the flow cytometry-based binding data, where TMP-1 and TMP-2 showed significant binding to the CCR5 transfected HOS.CCR5 cells (Fig. 3D). Thus, TMP-1 and TMP-2 were selected for further *in vitro* receptor binding studies.

The binding ability of the TMP-1 and TMP-2 was further validated in cells expressing varying levels of CCR5 (HOS.CCR5, PBMCs, THP-1) at different concentration. The cell population treated with various concentration of TMP-1 and TMP-2 showed a concentration-dependent binding in all three cell lines (Fig. 3B, C). The peptides showed the highest binding activity towards both THP-1 and HOS.CCR5 followed by PBMCs. This is in consistent with the immunostaining result, in which the expression level of CCR5 in PBMCs was low in comparison with the HOS.CCR5 and THP-1.

#### Inhibitory effect of TMP binding on CCR5 specific antibody binding

The specificity of TMP peptides was evaluated by pre-treating TMP-1 and TMP-2 with activated PBMCs,

followed by incubating the cells with anti-CCR5 monoclonal antibody. The pre-incubation of TMP-1 and TMP-2 with PBMCs inhibited the binding of T21/8 to CCR5 (Fig. 4). The cell population treated with TMP-1 and TMP-2 showed a significant reduction in the FITC fluorescence compared with that of cells treated with monoclonal antibody alone. The pre-treatment of TMP-1 reduced the FITC fluorescence up to 30%, whereas TMP-2 showed a 39% reduction in the FITC positive population. The reduction in the FITC fluorescence was more in cells treated with TMP-2, which suggests that TMP-2 is more specific to CCR5. The specific binding of variants to the cells harbouring the similar family of receptors confirmed the targetability of both TMP-1 and TMP-2.

#### Specific binding of variants

A competitive binding strategy was carried out to determine the specificity of TMP-1 and TMP-2 to CCR5 receptor, in which the cells were treated with rhodamine B-labelled peptides with or without excess RANTES. The percentage fluorescence associated with cells treated in the presence and absence of excess RANTES was examined using flow cytometry. The cells that were treated with both peptides and excess RANTES showed a notable reduction in the fluorescence compared with cells treated with variants alone. The reduction in fluorescence up to 20% was observed on the treatment with excess RANTES along with TMP-1. Similarly, the cells treated with TMP-2 along with RANTES showed a reduction in the fluorescence up to 34% (Fig. 5). The reduction in the binding of TMP-1 and TMP-2 to the CCR5 in the presence of excess RANTES confirmed that TMP-1 and TMP-2 were specifically targeting CCR5.



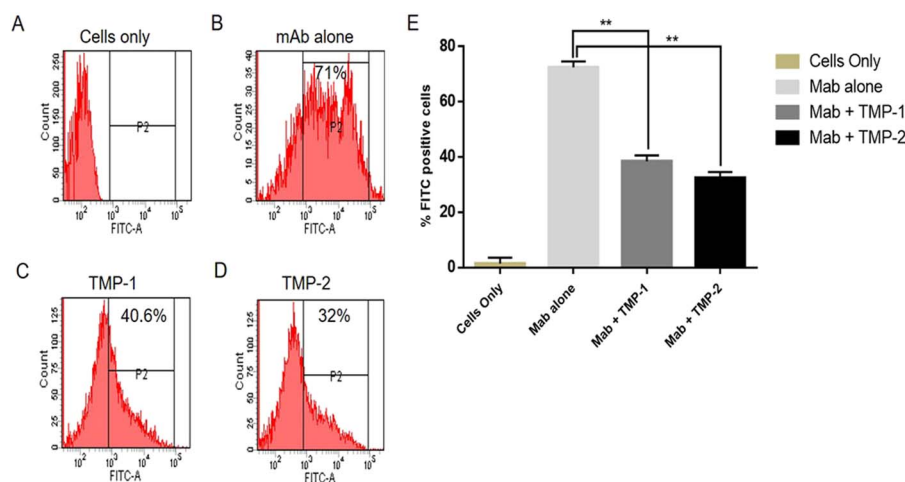


**Fig. 4. Inhibitory effect of TMP variants on T21/8 binding on PBMCs.** Histograms of cells pre-treated with peptide, followed by monoclonal antibody staining: (A) control, (B) mAb alone, (C) TMP-1 + mAb and (D) TMP-2 + mAb. The preincubation of 20  $\mu$ M TMP-1 and TMP-2 inhibited the binding of T21/8 (15  $\mu$ g/ml) to the CCR5 expressed on activated PBMCs. (E) The quantitative representation of the percentage of FITC-positive cells treated with Mab alone, Mab + TMP-1 and Mab + TMP-2. The data are expressed as mean  $\pm$  SD and \*\* represents statistical significance analysed by two-tailed unpaired Student's *t*-test ( $P < 0.01$ ).

#### Chemotactic migration assay

Chemokines are chemoattractant cytokines, involved in leukocyte activation and their migration. The responsiveness of CCR5 to the TMP-1 and TMP-2 was validated by measuring the chemotactic activity using transwell migration assay. Chemotaxis experiments were performed on HOS.CCR5 cells. TMP-1 and TMP-2 in the concentration range of 0.1–100  $\mu$ M were used. Specific agonist RANTES served as the positive control and cells treated with PBS served as the control. TMP-1 consistently appeared to be non-chemotactic at all the concentration tested, whereas TMP-2 at 100  $\mu$ M showed mild chemotactic response towards the CCR5 expressing cells. The migration of cells in response to RANTES was observed (Fig. 6).

The chemotaxis was further confirmed using agarose spot assay using HOS.CCR5 cells. A total of 0.5% agarose in PBS (negative control), RANTES (positive control) and TMP variants at different concentration were spotted in each well. Inconsistent with the quantitative transwell migration assay, cell migration was not observed under the agarose spot containing TMP-1. However, cell migration was observed under the spot containing TMP-2 at 100  $\mu$ M. The cells did not migrate under the agarose spot without a chemoattractant and was taken as the control and cell migration was observed in response to spots containing 10 nM RANTES (Supplementary Fig. 11).

#### CCR5 internalization assay

Activated PBMCs were used to investigate the CCR5 internalization mediated by TMP peptides. The cells were incubated with serum-free medium for 2 hours, followed by the treatment of peptides at the different concentration for 1 hour at 37°C to evaluate the internalization rate. The cells were then transferred to 4°C and the surface-bound variants were removed using acid stripping buffer, followed by PBS washes. The cell surface CCR5 was stained using T21/8 and secondary antibody. The TMP-2 induced 30% receptor internalization at a concentration of 10  $\mu$ M, whereas TMP-1 at concentration ranging from 0.1 to 100  $\mu$ M failed to mediate CCR5 internalization in PBMCs (Fig. 7).

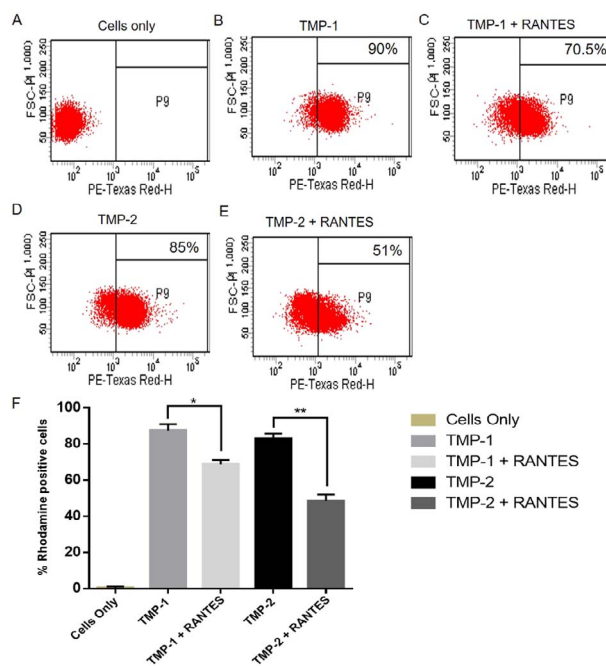


**Fig. 5. Competitive binding FACS analysis using excess RANTES.** The cells were treated with rhodamine-labelled TMP variants (20  $\mu$ M) in the presence or absence of 20-fold excess RANTES. The dot plot represents the following: (A) control (Cells only), (B) cells treated with TMP-1 alone, (C) TMP-1 + excess RANTES, (D) TMP-2 alone and (E) TMP-2 + excess RANTES. The reduction in the binding of TMP-1 and TMP-2 was observed in the presence of 20-fold excess RANTES. (F) The bar graph shows the percentage of rhodamine-positive cells with or without the treatment of RANTES followed by the addition of peptides. The data are expressed as mean  $\pm$  SD. The statistical significance of each treated condition is represented by \* and \*\*. Two-tailed unpaired Student's *t*-test values indicate statistical significance ( $*P < 0.05$  and  $**P < 0.01$ ).

#### Cytotoxic effects of TMP variants

Toxicity profiles of the TMP-1 and TMP-2 were analysed at 0.1, 1, 10 and 100  $\mu$ M concentration in HOS.CCR5 cells and PBMCs. TMP variants showed dose-dependent cytotoxic effect on both cells. At 100  $\mu$ M the variants



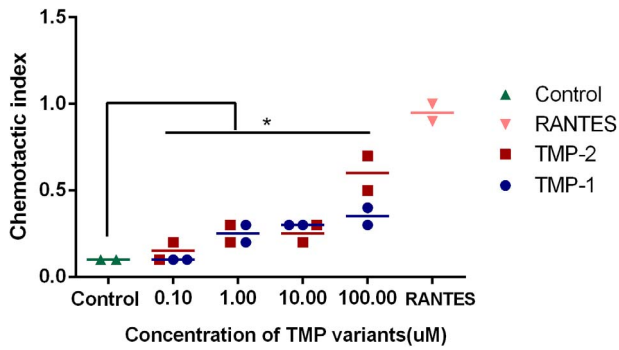


**Fig. 6. Chemotactic response of TMP variants at various concentration towards HOS.CCR5 cells was measured by transwell migration assay.** The chemotactic response of the HOS.CCR5 cells in the presence of TMP-1, TMP-2, RANTES (positive control) and PBS alone (control) was evaluated. TMP variants at different concentration (0.1, 0.1, 10, 100  $\mu$ M) and RANTES (10 nM) were added to the lower wells of the chamber and the HOS.CCR5 cells in FBS-free DMEM were added to the upper chamber and was incubated at 37°C for 4 hours. The filter was then removed and migrated cells were fixed and stained by crystal violet and counted. Data are presented as the mean number of cells counted in each field  $\pm$  SD of two independent experiments. One-way ANOVA followed by Dunnett's multiple comparison test was performed and the asterisk (\*) represents statistical significance in comparison with the control ( $P < 0.05$ ).

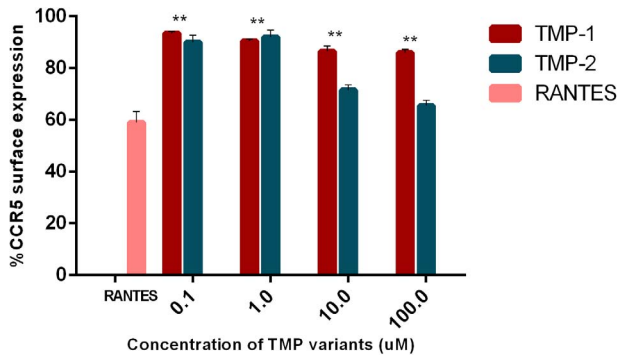


**Fig. 7. Internalization of CCR5 in PBMCs.** Dose-dependent effect on CCR5 internalization in PBMCs treated with TMP-2 was observed, whereas TMP-1 did not show any effect on CCR5 internalization. The results are presented as the mean  $\pm$  SD of two independent experiments on the same buffy coat. One-way ANOVA followed by Dunnett's multiple comparison test was performed, and the asterisk (\*\*) represents statistical significance in comparison with the control (RANTES) (\*\* $P < 0.01$ ).

displayed a similar level (40–50%) of toxicity against both the target cells (Fig. 8a, b).

The cytotoxicity of TMP variants towards human RBCs was also evaluated. At the highest concentration, the TMP-1 and TMP-2 showed only 13% and 20% of hemolysis, respectively (Fig. 8c).

## Discussion

The CCR5 chemokine receptor is involved in immune and inflammatory responses, as well as in the progression of various human diseases (7). The recent outbreak of COVID-19 put the world on hold and made the situation miserable due to the lack of appropriate therapeutic approaches. Subsequent studies have identified the involvement of several other receptors, including CCR5 in

COVID-19-related disease severity (85). The role of CCR5 in HIV-1 pathogenesis is well studied. Aside from its role in facilitating HIV-1 entry, CCR5 is involved in the formation of latent reservoirs, as majority of the viruses in the latent reservoir use CCR5 (86). In 2009, a case report showed that a Berlin patient, who had received the allogeneic stem cells from a homozygous CCR5 donor, achieved functional cure of HIV-1 infection, along with the reduction in the size of the viral reservoir (87, 88). The comprehensive analysis of his viral reservoir revealed that the HIV DNA levels were 7500-fold lower than those in patients receiving typical antiretroviral therapy (ART) (89). The involvement of CCR5 in the formation of drug resistant latent HIV-1 reservoir indicates the significance of targeting CCR5 beyond the perspective of entry inhibition. A rare group of individuals referred to as long-term nonprogressors, who have been able to maintain CD4+ T cell count and control the HIV-1 replication even in the absence of antiretroviral therapy, represent a model for functional cure (90). Several studies showed that the host factors and effective immunologic response plays crucial role in controlling the infection (91, 92). A recent study has shown that HIV-specific CD4+ T cells of controllers express low levels of CCR5, which inhibits the entry of HIV-1 (93). Thus, the CCR5 represents a target with multifaceted effects in the case of HIV-1 pathogenesis and disease progression. Studies using nonhuman primate as models for SIV infection showed that circulating CCR5+ memory CD4+ T cells from blood, mesenteric lymph nodes, mucosal surfaces such as gut, were selectively depleted in rapidly progressing SIV-infected monkeys during the initial phase of infection (99–101). These findings emphasized the importance of developing regimens that can achieve maximum virologic suppression during the early phase of infection. The combination of ART with CCR5 inhibitors may serve as an effective strategy to achieve cure, to prevent disease progression and to compensate for the shortcomings of existing therapy. Maraviroc is the only CCR5 inhibitor used in the treatment of naive and treatment-experienced HIV patients. Maraviroc-containing regimen achieved high rates of viral suppression and immunological responses in individuals who had failed to respond to previous regimens (94). Recent studies have shown that maraviroc can reactivate latent HIV *in vivo* (95). DAPTA is a short peptide derived from the V2 region of HIV gp120, which selectively targets CCR5. Monomeric DAPTA is 1000-fold more potent than maraviroc in inhibiting HIV-1 entry. The combination of ART along with DAPTA brought about an effective suppression of active HIV replication in the blood monocytes compared with peptide alone or by ART alone in individuals with stable plasma viremia (96–98).

The efforts to achieve CCR5 antagonism led to the development of various CCR5 targeting molecular entities, including chemokine analogues, small CCR5 molecule inhibitors and anti-CCR5 monoclonal antibodies (7). The peptide-based CCR5 inhibitors gained significant momentum, as peptide-based anti-viral therapeutics require evolutionary mutations or drastic changes in the viral structures for the virus to develop resistance against peptides (102). Unlike small molecule inhibitors, peptides can target protein-protein interactions more effectively because of their affinity for large protein surfaces (103). Chemokine variants represent the first generation of peptide-based CCR5

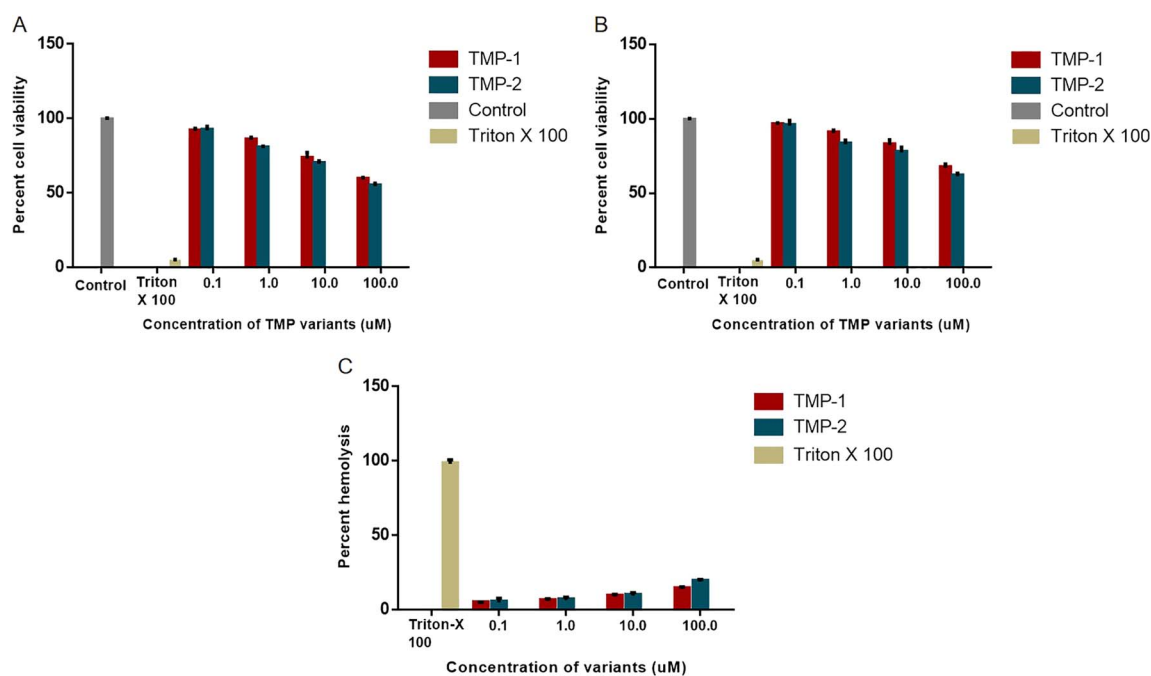


**Fig. 8.** Cytotoxic effects of TMP variants. TMP-1 and TMP-2 at different concentration were treated with (A) HOS.CCR5 cells and (B) PBMCs and the toxicity was evaluated by MTT assay after 48 hours of treatment. (C) Hemolytic effect of TMP variants, in which Triton-X 100 was taken as the positive control. Data are presented as mean  $\pm$  SD of two independent experiments.

inhibitors. The variants showed greater receptor specificity and selectivity than endogenous chemokine ligands. Few among the chemokine variants showed better anti-HIV-1 activity than that of maraviroc, and it has been reported that 5P12-RANTES resists the development of HIV-1-resistant strains (104, 105). Despite this, the clinical development of synthetic chemokine variants is difficult due to their high molecular weight, CCR5 agonist activity and their high cost of production. The generation of short peptides targeting CCR5 would be highly promising in this regard.

The idea for designing the peptide variants in this study came after paying close attention to the well-characterized HIV-1 gp120:CCR5 complex (106). A series of experiments depicted that certain residues or regions in the gp120 are involved in the host receptor binding and pathogenesis (77, 79, 80, 107, 108). Such an interaction interface could provide potential opportunity to develop inhibitors targeting the CCR5 receptor. This wealth of information provided the basis for selecting the primary sequence of peptide derived from the V3 crown region as the template (TMP-1) to generate the variants targeting CCR5. The validation of this approach has been obtained from a study conducted by Sakaida *et al.* (109). They showed that the peptides derived from the V3 loop of gp120 of naïve CD4-tropic HIV-1 interacted with its coreceptor CXCR4, independently of other variable regions or primary receptor CD4 (109). Molecular dynamic simulation was employed to design the TMP variants, as it is a widely used approach in studying ligand-receptor interaction and template-based drug designing (110). The key residues involved in TMP-1:CCR5 interaction were identified, and the binding energy of TMP-1 in complex with the receptor structure was obtained by molecular dynamic simulations. The TMP-2, TMP-3

and TMP-4 were designed based on the intermolecular interaction scores of individual amino acid residues of TMP-1 in complex with CCR5 receptor.

Several studies have indicated that the N-terminus, ECL2 and transmembrane helical regions 1, 2, 3 and 7 of CCR5 were critically involved in interacting with several small molecule CCR5 inhibitors, chemokine ligands and HIV-1 gp120 (75, 111–115). Consistent with this, the computationally derived complete structure of TMPs in complex with CCR5 showed that all the TMPs interacted with the aforementioned regions in the CCR5 receptor. Our analysis also showed that certain residues of CCR5 receptor such as Tyr14, Tyr15, Glu18, Pro19, Lys26, Leu33, Tyr37, Trp86, Tyr89, Ala90, Trp94, Leu104, Tyr108, Phe109, Gln170, Thr177, Cys178, Ser179, Ser180, His181, Phe182, Tyr184, Tyr187, Lys191, Ile198, Tyr251, Leu255, Asn258, Asp276, Met279, Gln280, Glu283 and Met287 were involved in TMP:CCR5 interaction. These residues have already been experimentally or computationally shown to interact with several small molecule CCR5 inhibitors, chemokine ligands and HIV-1 gp120 (106, 116–119). Such common residues in CCR5 that are being shared between a wide range of ligands represent key residues or regions to be targeted for developing CCR5 receptor antagonists or inhibitors.

The peptide variants were chemically synthesized using solid-phase peptide synthesis and were further labelled with rhodamine B to probe their *in vitro* binding ability. Synthetic peptides targeting CCR5 have been generated and shown to exhibit effective CCR5 blockade (120). The CCR5 targeting ability of the TMPs was examined in cell lines expressing varying levels of CCR5 receptor, as our goal was to generate variants with high receptor selectivity. Our *in vitro* findings demonstrated that the rhodamine

B-labelled TMP-1 and TMP-2 had higher binding ability as compared with TMP-3 and TMP-4. The promiscuous nature of the chemokine system often complicates the development of CCR5 specific ligands. The ability of the peptides to specifically target CCR5 was examined in PBMCs, which express various other chemokine receptors (83). The ability of the TMP-1 and TMP-2 to inhibit the binding of CCR5-specific monoclonal antibody in PBMCs, which harbour the pool of similar chemokine receptors, showed their effectiveness in targeting CCR5. The specificity of TMP-1 and TMP-2 was further confirmed using competitive binding experiment in the presence of excess RANTES.

In normal physiological conditions the binding of respective ligands to the CCR5 receptor leads to a rapid response such as receptor phosphorylation leading to calcium mobilization, chemotaxis and also the delayed response such as CCR5 internalization (121). The surface expression of CCR5 largely influences the ability of CCR5 in mediating disease development. In addition to the high-affinity receptor occupancy, CCR5 downmodulation was also suggested as an effective way to disable the cell surface distribution of CCR5. The PSC-RANTES, a variant generated from RANTES, which could mediate long-term internalization of CCR5, was reported to have potent anti-HIV-1 activity than other RANTES variants (122). Our, flow cytometry-based analyses showed that TMP-2-induced CCR5 receptor internalization, whereas TMP-1, with concentration ranging from 0.1 to 100  $\mu$ M, failed to mediate CCR5 internalization. The hallmark of the chemokine system is its ability to induce chemotaxis of target cells, and this aspect assumes great significance while targeting the chemokine system for therapeutic intervention (123). In this regard we performed chemotactic migration assay in responsive cells, and the data confirmed that TMPs were not chemotactic in nature.

In conclusion, the peptides used in this study have shown promising CCR5 inhibitory activity, in which the template TMP-1 showed high affinity towards CCR5 receptor, whereas TMP-2 showed CCR5 inhibition either by masking the exposed CCR5 or by inducing internalization of CCR5 receptor, without significant G protein-linked signalling activity. Further studies are needed to validate the effect of these peptides against those pathogens that hijack CCR5 for pathogenesis.

## Conclusion

Beyond the perspective of exploiting CCR5 as a target for inhibiting HIV-1 entry, being a highly redundant receptor having both positive and negative roles in the regulation of various physiological and pathological processes, CCR5 targeting represents a potential therapeutic strategy to combat several other infectious and non-infectious diseases. The significance of CCR5 targeting gained momentum again during the time of global COVID-19 pandemic, as the observation that CCR5 antagonism/blockade can be a potential therapeutic alternative to combat COVID infection, and the clinical trial of CCR5 antagonist cenicriviroc against COVID infection are underway (21, 22, 124). The study provided a preliminary hint regarding the efficacy of TMP variants in specifically targeting CCR5.

## Data availability statement

All the data presented in the manuscript is provided in the main text and the supplementary file.

## Supplementary Data

Supplementary Data are available at *JB* Online.

## Acknowledgements

We thank Dr. T. R. Santhosh Kumar and his team for their assistance in handling different cell lines. We thank Dr. Ajay Kumar for providing THP-1 cell line. We thank Dr. Sarah Jones, Dr. John Bernet Johnson and Dr. Deepak Chouhan, for critical advise and valuable suggestions. We thank Mr. Johny Philip, Ms. Smitha Devi and Mr. Manu N M for helping in setting up instruments and experiments in the lab. We also thank RGCB instrument facilities specially MALDI-MS facility, flowcytometry, microscopy (confocal microscope) and Mr. Tilak Prashad, Ms. Surabhi and Mr. Anuroop for technical assistance.

## Funding

This work was supported by the Department of Biotechnology [grant number no. BT/PR8835/NDB/52/61/20072]. Anju Krishnan Anitha received financial support from the Kerala State Council for Science Technology and Environment.

## Conflicts of Interest

The authors declare no conflict of interest.

## Author Contributions

Conceptualization, K.S.K and A.K.A.; methodology, A.K.A.; software, K.C.S.; validation, K.S.K., A.K.A., P.N. and N.A.; formal analysis, K.S.K and A.K.A.; investigation, K.S.K.; resources, K.S.K.; data curation, K.S.K and A.K.A.; writing (original draft preparation), A.K.A.; writing (review and editing), K.S.K and A.K.A.; visualization, K.S.K.; supervision, K.S.K.; funding acquisition, K.S.K. All authors have read and agreed to the published version of the manuscript.

## REFERENCES

1. Corbeau, P., and Reynes, J. (2009) CCR5 antagonism in HIV infection: ways, effects, and side effects. *AIDS* **23**, 1931–1943
2. Rottman, J.B., Ganley, K.P., Williams, K., Wu, L., Mackay, C.R., and Ringler, D.J. (1997) Cellular localization of the chemokine receptor CCR5. Correlation to cellular targets of HIV-1 infection. *Am. J. Pathol.* **151**, 1341–1351
3. Chávez, J.H., França, R.F., Oliveira, C.J., de Aquino, M.T., Farias, K.J., Machado, P.R., de Oliveira, T.F., Yokosawa, J., Soares, E.G., and da Silva, J.S. (2013) Influence of the CCR-5/MIP-1  $\alpha$  axis in the pathogenesis of Rocio virus encephalitis in a mouse model. *Am. J. Trop. Med. Hyg.* **89**, 1013–1018



4. Badolato-Corrêa, J., Sánchez-Arcila, J.C., Alves de Souza, T.M., Santos Barbosa, L., Conrado Guerra Nunes, P., da Rocha Queiroz Lima, M., Gandini, M., Bispo de Filippis, A.M., Venâncio da Cunha, R., Leal de Azeredo, E., and de-Oliveira-Pinto, L.M. (2018) Human T cell responses to dengue and Zika virus infection compared to dengue/Zika coinfection. *Immun. Inflamm. Dis.* **6**, 194–206
5. Zachova, K., Kosztyu, P., Zadrzil, J., Matousovic, K., Vondrak, K., Hubacek, P., Kostovcikova, K., Hogenova, H.T., Mestecky, J., and Raska, M. (2020) Multiparametric flow cytometry analysis of peripheral blood B cell trafficking differences among Epstein–Barr virus infected and uninfected subpopulations. *Biomed. Pap. Med. Fac. Univ. Palacky Olomouc Czech. Repub.* **164**, 247–254
6. Rajan, D., McCracken, C.E., Kopleman, H.B., Kyu, S.Y., Lee, F.E.-H., Lu, X., and Anderson, L.J. (2014) Human rhinovirus induced cytokine/chemokine responses in human airway epithelial and immune cells. *PLoS One* **9**, e114322
7. Vangelista, L., and Vento, S. (2018) The expanding therapeutic perspective of CCR5 blockade. *Front. Immunol.* **8**, 1981
8. Necula, D., Riviere-Cazaux, C., Shen, Y., and Zhou, M. (2021) Insight into the roles of CCR5 in learning and memory in normal and disordered states. *Brain Behav. Immun.* **92**, 1–9
9. Martin-Blondel, G., Brassat, D., Bauer, J., Lassmann, H., and Liblau, R.S. (2016) CCR5 blockade for neuroinflammatory diseases—beyond control of HIV. *Nat. Rev. Neurol.* **12**, 95–105
10. Cui, L.-Y., Chu, S.-F., and Chen, N.-H. (2020) The role of chemokines and chemokine receptors in multiple sclerosis. *Int. Immunopharmacol.* **83**, 106314
11. Aldinucci, D., and Casagrande, N. (2018) Inhibition of the CCL5/CCR5 axis against the progression of gastric cancer. *Int. J. Mol. Sci.* **19**, 1477
12. Jiao, X., Nawab, O., Patel, T., Kossenkov, A.V., Halama, N., Jaeger, D., and Pestell, R.G. (2019) Recent advances targeting CCR5 for cancer and its role in immuno-oncology. *Cancer Res.* **79**, 4801–4807
13. Aldinucci, D., and Colombatti, A. (2014) The inflammatory chemokine CCL5 and cancer progression. *Mediat. Inflamm.* **2014**, 1–12
14. Prahalad, S. (2006) Negative association between the chemokine receptor CCR5-Δ32 polymorphism and rheumatoid arthritis: a meta-analysis. *Genes Immun.* **7**, 264–268
15. Szalai, C., Duba, J., Prohászka, Z., Kalina, Á., Szabó, T., Nagy, B., Horváth, L., and Császár, A. (2001) Involvement of polymorphisms in the chemokine system in the susceptibility for coronary artery disease (CAD). Coincidence of elevated Lp (a) and MCP-1—2518 G/G genotype in CAD patients. *Atherosclerosis* **158**, 233–239
16. Liu, R., Paxton, W.A., Choe, S., Ceradini, D., Martin, S.R., Horuk, R., Mac Donald, M.E., Stuhlmann, H., Koup, R.A., and Landau, N.R. (1996) Homozygous defect in HIV-1 coreceptor accounts for resistance of some multiply-exposed individuals to HIV-1 infection. *Cell* **86**, 367–377
17. Rustemoglu, A., Ekinci, D., Nursal, A.F., Barut, S., Duygu, F., and Günal, Ö. (2017) The possible role of CCR5Δ32 mutation in Crimean-Congo hemorrhagic fever infection. *J. Med. Virol.* **89**, 1714–1719
18. Rahbar, R., Murooka, T.T., Hinek, A.A., Galligan, C.L., Sassano, A., Yu, C., Srivastava, K., Platanius, L.C., and Fish, E.N. (2006) Vaccinia virus activation of CCR5 invokes tyrosine phosphorylation signaling events that support virus replication. *J. Virol.* **80**, 7245–7259
19. Rahbar, R., Murooka, T.T., and Fish, E.N. (2009) Role for CCR5 in dissemination of vaccinia virus in vivo. *J. Virol.* **83**, 2226–2236
20. Alonzo, F., III, Kozhaya, L., Rawlings, S.A., Reyes-Robles, T., DuMont, A.L., Myszka, D.G., Landau, N.R., Unutmaz, D., and Torres, V.J. (2013) CCR5 is a receptor for Staphylococcus aureus leukotoxin ED. *Nature* **493**, 51–55
21. Okamoto, M., Toyama, M., and Baba, M. (2020) The chemokine receptor antagonist cenicriviroc inhibits the replication of SARS-CoV-2 in vitro. *Antivir. Res.* **182**, 104902
22. Agresti, N., Lalezari, J.P., Amodeo, P.P., Mody, K., Mosher, S.F., Seethamraju, H., Kelly, S.A., Pourhassan, N.Z., Suduth, C.D., Bovinet, C., ElSharkawi, A.E., Patterson, B.K., Stephen, R., Sacha, J.B., Wu, H.L., Gross, S.A., and Dhody, K. (2021) Disruption of CCR5 signaling to treat COVID-19-associated cytokine storm: case series of four critically ill patients treated with leronlimab. *J. Transl. Autoimmun.* **4**, 100083
23. Costela-Ruiz, V.J., Illescas-Montes, R., Puerta-Puerta, J.M., Ruiz, C., and Melguizo-Rodríguez, L. (2020) SARS-CoV-2 infection: the role of cytokines in COVID-19 disease. *Cytokine Growth Factor Rev.* **54**, 62–75
24. Mack, M., Luckow, B., Nelson, P.J., Cihak, J., Simmons, G., Clapham, P.R., Signoret, N., Marsh, M., Stangassinger, M., Borlat, F., Wells, T.N.C., Schlöndorff, D., and Proudfoot, A.E.I. (1998) Aminoxy-pentane-RANTES induces CCR5 internalization but inhibits recycling: a novel inhibitory mechanism of HIV infectivity. *J. Exp. Med.* **187**, 1215–1224
25. Kawamura, T., Bruce, S.E., Abraha, A., Sugaya, M., Hartley, O., Offord, R.E., Arts, E.J., Zimmerman, P.A., and Blauvelt, A. (2004) PSC-RANTES blocks R5 human immunodeficiency virus infection of Langerhans cells isolated from individuals with a variety of CCR5 diplotypes. *J. Virol.* **78**, 7602–7609
26. Redwine, L.S., Pert, C.B., Rone, J.D., Nixon, R., Vance, M., Sandler, B., Lumpkin, M.D., Dieter, D.J., and Ruff, M.R. (1999) Peptide T blocks GP120/CCR5 chemokine receptor-mediated chemotaxis. *Clin. Immunol.* **93**, 124–131
27. Ray, N. (2008) Maraviroc in the treatment of HIV infection. *Drug Des. Dev. Ther.* **2**, 151
28. Sierra-Madero, J.G., Ellenberg, S.S., Rassool, M.S., Tierney, A., Belaunzarán-Zamudio, P.F., López-Martínez, A., Piñeirúa-Menéndez, A., Montaner, L.J., Azzoni, L., Benítez, C.R., Sereti, I., Andrade-Villanueva, J., Mosqueda-Gómez, J.L., Rodríguez, B., Sanne, I., Lederman, M.M., and CADIRIS Study Team (2014) Effect of the CCR5 antagonist maraviroc on the occurrence of immune reconstitution inflammatory syndrome in HIV (CADIRIS): a double-blind, randomised, placebo-controlled trial. *The Lancet HIV* **1**, e60–e67
29. Ochoa-Callejero, L., Pérez-Martínez, L., Rubio-Mediavilla, S., Oteo, J.A., Martínez, A., and Blanco, J.R. (2013) Maraviroc, a CCR5 antagonist, prevents development of hepatocellular carcinoma in a mouse model. *PLoS One* **8**, e53992
30. Halvorsen, E., Hamilton, M., Young, A., Wadsworth, B., LePard, N., Lee, H., Firmino, N., Collier, J., and Bennewith, K. (2016) Maraviroc decreases CCL8-mediated migration of CCR5+ regulatory T cells and reduces metastatic tumor growth in the lungs. *Oncoimmunology* **5**, e1150398
31. Latinovic, O., Kuruppu, J., Davis, C., Le, N., and Heredia, A. (2009) Pharmacotherapy of HIV-1 infection: focus on CCR5 antagonist maraviroc. *Clin. Med. Ther.* **1**, CMT.S2365
32. Gutierrez, M.D.M., Mur, I., Mateo, M.G., Vidal, F., and Domingo, P. (2021) Pharmacological considerations for the treatment of COVID-19 in people living with HIV (PLWH). *Expert. Opin. Pharmacother.* **22**, 1127–1141
33. Friedman, S., Sanyal, A., Goodman, Z., Lefebvre, E., Gottwald, M., Fischer, L., and Ratziu, V. (2016) Efficacy and safety study of cenicriviroc for the treatment of non-alcoholic steatohepatitis in adult subjects with liver fibrosis:

- CENTAUR phase 2b study design. *Contemp. Clin. Trials* **47**, 356–365
34. Anstee, Q.M., Neuschwander-Tetri, B.A., Wong, V.W.-S., Abdelmalek, M.F., Younossi, Z.M., Yuan, J., Pecoraro, M.L., Seyedkazemi, S., Fischer, L., Bedossa, P., Goodman, Z., Alkhoury, N., Tacke, F., and Sanyal, A. (2020) Cenicriviroc for the treatment of liver fibrosis in adults with nonalcoholic steatohepatitis: AURORA phase 3 study design. *Contemp. Clin. Trials* **89**, 105922
  35. Baba, M., Takashima, K., Miyake, H., Kanzaki, N., Teshima, K., Wang, X., Shiraiishi, M., and Iizawa, Y. (2005) TAK-652 inhibits CCR5-mediated human immunodeficiency virus type 1 infection in vitro and has favorable pharmacokinetics in humans. *Antimicrob. Agents Chemother.* **49**, 4584–4591
  36. Berlin, C.-U. (2020) Charité trial of Cenicriviroc (CVC) treatment for COVID-19 patients.
  37. Qi, B., Fang, Q., Liu, S., Hou, W., Li, J., Huang, Y., and Shi, J. (2020) Advances of CCR5 antagonists: from small molecules to macromolecules. *Eur. J. Med. Chem.* **208**, 112819
  38. Olson, W.C., Rabut, G.E., Nagashima, K.A., Tran, D.N., Anselma, D.J., Monard, S.P., Segal, J.P., Thompson, D.A., Kajumo, F., Guo, Y., Moore, J.P., Maddon, P.J., and Dragic, T. (1999) Differential inhibition of human immunodeficiency virus type 1 fusion, gp120 binding, and CC-chemokine activity by monoclonal antibodies to CCR5. *J. Virol.* **73**, 4145–4155
  39. Jacobson, J.M., Lalezari, J.P., Thompson, M.A., Fichtenbaum, C.J., Saag, M.S., Zingman, B.S., D'Ambrosio, P., Stambler, N., Rotshteyn, Y., Marozsan, A.J., Maddon, P.J., Morris, S.A., and Olson, W.C. (2010) Phase 2a study of the CCR5 monoclonal antibody PRO 140 administered intravenously to HIV-infected adults. *Antimicrob. Agents Chemother.* **54**, 4137–4142
  40. Cristofanilli, M., Dolezal, M., Lalezari, J., Rui, H., Patterson, B., Tang, C.-M., Adams, D., Zhang, Q., Kazempour, K., and Pourhassan, N. (2020) Abstract CT233: phase Ib/II study of leronlimab (PRO 140) combined with carboplatin in CCR5+ mTNBC patients. *AACR*. **80**, CT233–CT233
  41. Skendelas, J., Phan, D., Caputo, V., Stryker, K., Ahmed, S., Philippsborn, P., Thalappillil, J., Scheinin, S., and Seethamraju, H. (2021) Novel CCR5 antagonist for the treatment of mild-moderate COVID-19 infection after lung transplant. *J. Heart Lung Transplant.* **40**, S315
  42. Starcich, B.R., Hahn, B.H., Shaw, G.M., McNeely, P.D., Modrow, S., Wolf, H., Parks, E.S., Parks, W.P., Josephs, S.F., Gallo, R.C., and Wong-Staal, F. (1986) Identification and characterization of conserved and variable regions in the envelope gene of HTLV-III/LAV, the retrovirus of AIDS. *Cell* **45**, 637–648
  43. Leonard, C.K., Spellman, M.W., Riddle, L., Harris, R.J., Thomas, J.N., and Gregory, T. (1990) Assignment of intrachain disulfide bonds and characterization of potential glycosylation sites of the type 1 recombinant human immunodeficiency virus envelope glycoprotein (gp120) expressed in Chinese hamster ovary cells. *J. Biol. Chem.* **265**, 10373–10382
  44. Xiang, S.-H., Finzi, A., Pacheco, B., Alexander, K., Yuan, W., Rizzuto, C., Huang, C.-C., Kwong, P.D., and Sodroski, J. (2010) A V3 loop-dependent gp120 element disrupted by CD4 binding stabilizes the human immunodeficiency virus envelope glycoprotein trimer. *J. Virol.* **84**, 3147–3161
  45. Cardozo, T., Kimura, T., Philpott, S., Weiser, B., Burger, H., and Zolla-Pazner, S. (2007) Structural basis for coreceptor selectivity by the HIV type 1 V3 loop. *AIDS Res. Hum. Retrovir.* **23**, 415–426
  46. Foda, M., Harada, S., and Maeda, Y. (2001) Role of V3 independent domains on a dualtropic human immunodeficiency virus type 1 (HIV-1) envelope gp120 in CCR5 coreceptor utilization and viral infectivity. *Microbiol. Immunol.* **45**, 521–530
  47. Hartley, O., Klasse, P.J., Sattentau, Q.J., and Moore, J.P. (2005) V3: HIV's switch-hitter. *AIDS Res.* **21**, 171–189
  48. Hongjaisee, S., Braibant, M., Barin, F., Ngo-Giang-Huong, N., Sirirungsri, W., and Samleerat, T. (2017) Effect of amino acid substitutions within the V3 region of HIV-1 CRF01\_AE on interaction with CCR5-coreceptor. *AIDS Res. Hum. Retrovir.* **33**, 946–951
  49. Huang, C.-C., Tang, M., Zhang, M.-Y., Majeed, S., Montabana, E., Stanfield, R.L., Dimitrov, D.S., Korber, B., Sodroski, J., Wilson, I.A., Wyatt, R., and Kwong, P.D. (2005) Structure of a V3-containing HIV-1 gp120 core. *Science* **310**, 1025–1028
  50. Jiang, X., Burke, V., Totrov, M., Williams, C., Cardozo, T., Gorny, M.K., Zolla-Pazner, S., and Kong, X.-P. (2010) Conserved structural elements in the V3 crown of HIV-1 gp120. *Nat. Struct. Mol. Biol.* **17**, 955–961
  51. Moore, J.P., and Nara, P.L. (1991) The role of the V3 loop of gp 120 in HIV infection. *AIDS* **5**, 21–34
  52. O'Brien, W.A., Koyanagi, Y., Namazie, A., Zhao, J.-Q., Diagne, A., Zack, J.A., and Chen, I.S. (1990) HIV-1 tropism for mononuclear phagocytes can be determined by regions of gp120 outside the CD4-binding domain. *Nature* **348**, 69–73
  53. Shioda, T., Levy, J.A., and Cheng-Mayer, C. (1991) Macrophage and T cell-line tropisms of HIV-1 are determined by specific regions of the envelope gp! 20 gene. *Nature* **349**, 167–169
  54. Trujillo, J.R., Wang, W.-K., Lee, T.-H., and Essex, M. (1996) Identification of the envelope V3 loop as a determinant of a CD4-negative neuronal cell tropism for HIV-1. *Virology* **217**, 613–617
  55. Westervelt, P., Trowbridge, D., Epstein, L., Blumberg, B., Li, Y., Hahn, B., Shaw, G., Price, R., and Ratner, L. (1992) Macrophage tropism determinants of human immunodeficiency virus type 1 in vivo. *J. Virol.* **66**, 2577–2582
  56. LaRosa, G.J., Davide, J.P., Weinhold, K., Waterbury, J.A., Profy, A.T., Lewis, J.A., Langlois, A.J., Dreesman, G.R., Boswell, R.N., Shadduck, P., Holley, L.H., Karplus, M., Bolognesi, D.P., Matthews, T.J., Emini, E.A., and Putney, S.D. (1990) Conserved sequence and structural elements in the HIV-1 principal neutralizing determinant. *Science* **249**, 932–935
  57. LaRosa, G.J., Weinhold, K., Profy, A.T., Langlois, A.J., Dreesman, G.R., Boswell, R.N., Shadduck, P., Bolognesi, D.P., Matthews, T.J., Emini, E.A., and Putney, S.D. (1991) Conserved sequence and structural elements in the HIV-1 principal neutralizing determinant: further clarifications. *Science* **253**, 1146–1147
  58. Javaherian, K., Langlois, A.J., McDanal, C., Ross, K.L., Eckler, L.I., Jellis, C.L., Profy, A.T., Rusche, J.R., Bolognesi, D.P., and Putney, S.D. (1989) Principal neutralizing domain of the human immunodeficiency virus type 1 envelope protein. *Proc. Natl. Acad. Sci. U. S. A.* **86**, 6768–6772
  59. Cormier, E.G., and Dragic, T. (2002) The crown and stem of the V3 loop play distinct roles in human immunodeficiency virus type 1 envelope glycoprotein interactions with the CCR5 coreceptor. *J. Virol.* **76**, 8953–8957
  60. Kleiveland, C.R. (2015) Peripheral blood mononuclear cells in *The Impact of Food Bioactives on Health*. pp161–167
  61. Suphaphiphat, P., Thitithanyanont, A., Paca-Uccaralertkun, S., Essex, M., and Lee, T.-H. (2003) Effect of amino acid substitution of the V3 and bridging sheet residues in human immunodeficiency virus type 1 subtype C gp120 on CCR5 utilization. *J. Virol.* **77**, 3832–3837
  62. de Victoria, A.L., Tamamis, P., Kieslich, C.A., and Morikis, D. (2012) Insights into the structure, correlated motions, and

- electrostatic properties of two HIV-1 gp120 V3 loops. *PLoS One* **7**, e49925
63. Vranken, W.F., Budesinsky, M., Fant, F., Boulez, K., and Borremans, F.A. (1995) The complete consensus V3 loop peptide of the envelope protein gp120 of HIV-1 shows pronounced helical character in solution. *Fed. Eur. Biochem. Soc. Lett.* **374**, 117–121
  64. Tan, Q., Zhu, Y., Li, J., Chen, Z., Han, G.W., Kufareva, I., Li, T., Ma, L., Fenalti, G., Li, J., Zhang, W., Xie, X., Yang, H., Jiang, H., Cherezov, V., Liu, H., Stevens, R.C., Zhao, Q., and Wu, B. (2013) Structure of the CCR5 chemokine receptor–HIV entry inhibitor maraviroc complex. *Science* **341**, 1387–1390
  65. Pronk, S., Páll, S., Schulz, R., Larsson, P., Bjelkmar, P., Apostolov, R., Shirts, M.R., Smith, J.C., Kasson, P.M., van der Spoel, D., Hess, B., and Lindahl, E. (2013) GROMACS 4.5: a high-throughput and highly parallel open source molecular simulation toolkit. *Bioinformatics* **29**, 845–854
  66. Kumari, R., Kumar, R., Consortium, O.S.D.D., and Lynn, A. (2014) g\_mmpbsa—white medium square a GROMACS tool for high-throughput MM-PBSA calculations. *J. Chem. Inf. Model.* **54**, 1951–1962
  67. Pierce, B.G., Hourai, Y., and Weng, Z. (2011) Accelerating protein docking in ZDOCK using an advanced 3D convolution library. *PLoS One* **6**, e24657
  68. Ahmed, M., Basheer, H.A., Ayuso, J.M., Ahmet, D., Mazzini, M., Patel, R., Shnyder, S.D., Vinader, V., and Afarinkia, K. (2017) Agarose spot as a comparative method for in situ analysis of simultaneous chemotactic responses to multiple chemokines. *Sci. Rep.* **7**, 1–11
  69. Liebick, M., Schläger, C., and Oppermann, M. (2016) Analysis of chemokine receptor trafficking by site-specific biotinylation. *PLoS One* **11**, e0157502
  70. Li, N., Hill, K.S., and Elferink, L.A. (2008) Analysis of receptor tyrosine kinase internalization using flow cytometry in *Membrane Trafficking*. pp305–317 Humana Press, Totowa, NJ
  71. Lue, H., Dewor, M., Bernhagen, J., and Weber, C. (2007) Receptor internalization assay to probe for agonist binding to CXCR2. nprot.2007.213
  72. Van Meerloo, J., Kaspers, G.J., and Cloos, J. (2011) Cell sensitivity assays: the MTT assay in *Cancer Cell Culture*. pp 237–245 Springer, Humana Press
  73. Dragic, T., Trkola, A., Lin, S.W., Nagashima, K.A., Kajumo, F., Zhao, L., Olson, W.C., Wu, L., Mackay, C.R., Allaway, G.P., Sakmar, T.P., Moore, J.P., and Maddon, P.J. (1998) Amino-terminal substitutions in the CCR5 coreceptor impair gp120 binding and human immunodeficiency virus type 1 entry. *J. Virol.* **72**, 279–285
  74. Melikyan, G.B., Platt, E.J., and Kabat, D. (2007) The role of the N-terminal segment of CCR5 in HIV-1 Env-mediated membrane fusion and the mechanism of virus adaptation to CCR5 lacking this segment. *Retrovirology* **4**, 55–14
  75. Farzan, M., Choe, H., Vaca, L., Martin, K., Sun, Y., Desjardins, E., Ruffing, N., Wu, L., Wyatt, R., Gerard, N., Gerard, C., and Sodroski, J. (1998) A tyrosine-rich region in the N terminus of CCR5 is important for human immunodeficiency virus type 1 entry and mediates an association between gp120 and CCR5. *J. Virol.* **72**, 1160–1164
  76. Wang, W.-K., Dudek, T., Essex, M., and Lee, T.-H. (1999) Hypervariable region 3 residues of HIV type 1 gp120 involved in CCR5 coreceptor utilization: therapeutic and prophylactic implications. *Proc. Natl. Acad. Sci. U. S. A.* **96**, 4558–4562
  77. Cormier, E.G., Tran, D.N., Yukhayeva, L., Olson, W.C., and Dragic, T. (2001) Mapping the determinants of the CCR5 amino-terminal sulfopeptide interaction with soluble human immunodeficiency virus type 1 gp120-CD4 complexes. *Journal of virology* **75**, 5541–5549
  78. Yuriev, E., Holien, J., and Ramsland, P.A. (2015) Improvements, trends, and new ideas in molecular docking: 2012–2013 in review. *J. Mol. Recognit.* **28**, 581–604
  79. Su, J., Palm, A., Wu, Y., Sandin, S., Hoglund, S., and Vahlne, A. (2000) Deletion of the GPG motif in the HIV type 1 V3 loop does not abrogate infection in all cells. *AIDS Res. Hum. Retrovir.* **16**, 37–48
  80. Grimaila, R.J., Fuller, B.A., Rennert, P.D., Nelson, M., Hammarskjöld, M., Potts, B., Murray, M., Putney, S., and Gray, G. (1992) Mutations in the principal neutralization determinant of human immunodeficiency virus type 1 affect syncytium formation, virus infectivity, growth kinetics, and neutralization. *Journal of virology* **66**, 1875–1883
  81. Stanfield, R., Cabezas, E., Satterthwait, A., Stura, E., Profy, A., and Wilson, I. (1999) Dual conformations for the HIV-1 gp120 V3 loop in complexes with different neutralizing fabs. *Structure* **7**, 131–142
  82. Cristofaro, D. (1999) CCR5 and CXCR4 chemokine receptor expression and  $\beta$ -chemokine production during early T cell repopulation induced by highly active anti-retroviral therapy. *Clin. Exp. Immunol.* **118**, 87–94
  83. Nieto, J.C., Cantó, E., Zamora, C., Ortiz, M.A., Juárez, C., and Vidal, S. (2012) Selective loss of chemokine receptor expression on leukocytes after cell isolation. *PLoS One* **7**, e31297
  84. Konopka, K., and Düzgüneş, N. (2002) Expression of CD4 controls the susceptibility of THP-1 cells to infection by R5 and X4 HIV type 1 isolates. *AIDS Res. Hum. Retrovir.* **18**, 123–131
  85. Mehlotra, R.K. (2020) Chemokine receptor gene polymorphisms and COVID-19: could knowledge gained from HIV/AIDS be important? *Infect. Genet. Evol.* **85**, 104512
  86. Pierson, T., Hoffman, T.L., Blankson, J., Finzi, D., Chadwick, K., Margolick, J.B., Buck, C., Siliciano, J.D., Doms, R.W., and Siliciano, R.F. (2000) Characterization of chemokine receptor utilization of viruses in the latent reservoir for human immunodeficiency virus type 1. *J. Virol.* **74**, 7824–7833
  87. Hütter, G., Nowak, D., Mossner, M., Ganepola, S., Müßig, A., Allers, K., Schneider, T., Hofmann, J., Kücherer, C., Blau, O., Blau, I.W., Hofmann, W.K., and Thiel, E. (2009) Long-term control of HIV by CCR5 Delta32/Delta32 stem-cell transplantation. *N. Engl. J. Med.* **360**, 692–698
  88. Allers, K., Hütter, G., Hofmann, J., Loddenkemper, C., Rieger, K., Thiel, E., and Schneider, T. (2011) Evidence for the cure of HIV infection by CCR5 $\Delta$ 32/ $\Delta$ 32 stem cell transplantation. *Blood* **117**, 2791–2799
  89. Yukl, S.A., Boritz, E., Busch, M., Bentsen, C., Chun, T.-W., Douek, D., Eisele, E., Haase, A., Ho, Y.-C., Hütter, G., Justement, J.S., Keating, S., Lee, T.H., Li, P., Murray, D., Palmer, S., Pilcher, C., Pillai, S., Price, R.W., Rothenberger, M., Schacker, T., Siliciano, J., Siliciano, R., Sinclair, E., Strain, M., Wong, J., Richman, D., and Deeks, S.G. (2013) Challenges in detecting HIV persistence during potentially curative interventions: a study of the Berlin patient. *PLoS Pathog.* **9**, e1003347
  90. Lambotte, O., Boufassa, F., Madec, Y., Nguyen, A., Goujard, C., Meyer, L., Rouzioux, C., Venet, A., Delfraissy, J.-F., and SEROCO-HEMOCO Study Group (2005) HIV controllers: a homogeneous group of HIV-1—infected patients with spontaneous control of viral replication. *Clin. Infect. Dis.* **41**, 1053–1056
  91. Blankson, J.N., Bailey, J.R., Thayil, S., Yang, H.-C., Lassen, K., Lai, J., Gandhi, S.K., Siliciano, J.D., Williams, T.M., and Siliciano, R.F. (2007) Isolation and characterization of replication-competent human immunodeficiency virus type 1 from a subset of elite suppressors. *J. Virol.* **81**, 2508–2518



92. Boppana, S., and Goepfert, P. (2018) Understanding the CD8 T-cell response in natural HIV control. *F1000Research* **7**.
93. Claireaux, M., Robinot, R., Kervevan, J., Patgaonkar, M., Staropoli, I., Brelot, A., Nouël, A., Gellenoncourt, S., Tang, X., Héry, M., Volant, S., Perthame, E., Avettand-Fenoël, V., Buchrieser, J., Cokelaer, T., Bouchier, C., Ma, L., Boufassa, F., Hendou, S., Libri, V., Hasan, M., Zucman, D., de Truchis, P., Schwartz, O., Lambotte, O., and Chakrabarti, L.A. (2022) Low CCR5 expression protects HIV-specific CD4+ T cells of elite controllers from viral entry. *Nat. Commun.* **13**, 1–19
94. Potard, V., Reynes, J., Ferry, T., Aubin, C., Finkielstejn, L., Yazdanpanah, Y., Costagliola, D., and CO4, F.A. (2015) Durability and effectiveness of Maraviroc-containing regimens in HIV-1-infected individuals with virological failure in routine clinical practice. *PLoS One* **10**, e0144746
95. López-Huertas, M.R., Gutiérrez, C., Madrid-Elena, N., Hernández-Novoa, B., Olalla-Sierra, J., Plana, M., Delgado, R., Rubio, R., Muñoz-Fernández, M.Á., and Moreno, S. (2020) Prolonged administration of maraviroc reactivates latent HIV in vivo but it does not prevent antiretroviral-free viral rebound. *Sci. Rep.* **10**, 1–13
96. Polianova, M.T., Ruscetti, F.W., Pert, C.B., and Ruff, M.R. (2005) Chemokine receptor-5 (CCR5) is a receptor for the HIV entry inhibitor peptide T (DAPTA). *Antivir. Res.* **67**, 83–92
97. Polianova, M.T., Ruscetti, F.W., Pert, C.B., Tractenberg, R.E., Leoung, G., Strang, S., and Ruff, M.R. (2003) Antiviral and immunological benefits in HIV patients receiving intranasal peptide T (DAPTA). *Peptides* **24**, 1093–1098
98. Venanzi Rullo, E., Ceccarelli, M., Condorelli, F., Facciola, A., Visalli, G., D'Aleo, F., Paolucci, I., Cacopardo, B., Pinzone, M.R., and Di Rosa, M. (2019) Investigational drugs in HIV: pros and cons of entry and fusion inhibitors. *Mol. Med. Rep.* **19**, 1987–1995
99. Nishimura, Y., Igarashi, T., Donau, O.K., Buckler-White, A., Buckler, C., Lafont, B.A., Goeken, R.M., Goldstein, S., Hirsch, V.M., and Martin, M.A. (2004) Highly pathogenic SHIVs and SIVs target different CD4+ T cell subsets in rhesus monkeys, explaining their divergent clinical courses. *PNAS Nexus* **101**, 12324–12329
100. Li, Q., Duan, L., Estes, J.D., Ma, Z.-M., Rourke, T., Wang, Y., Reilly, C., Carlis, J., Miller, C.J., and Haase, A.T. (2005) Peak SIV replication in resting memory CD4+ T cells depletes gut lamina propria CD4+ T cells. *Nature* **434**, 1148–1152
101. Mattapallil, J.J., Douek, D.C., Hill, B., Nishimura, Y., Martin, M., and Roederer, M. (2005) Massive infection and loss of memory CD4+ T cells in multiple tissues during acute SIV infection. *Nature* **434**, 1093–1097
102. Shi, S., Nguyen, P.K., Cabral, H.J., Diez-Barroso, R., Derry, P.J., Kanahara, S.M., and Kumar, V.A. (2016) Development of peptide inhibitors of HIV transmission. *Bioact. Mater.* **1**, 109–121
103. Belvisi, L., D'Andrea, L.D., and Jiménez, M.A. (2021) Peptides targeting protein-protein interactions: methods and applications. *Front. Mol. Biosci.* **8**.
104. Gaertner, H., Cerini, F., Escola, J.-M., Kuenzi, G., Melotti, A., Offord, R., Rossitto-Borlat, I., Nedellec, R., Salkowitz, J., Gorochov, G., Mosier, D., and Hartley, O. (2008) Highly potent, fully recombinant anti-HIV chemokines: reengineering a low-cost microbicide. *Proc. Natl. Acad. Sci. U. S. A.* **105**, 17706–17711
105. Nedellec, R., Coetzer, M., Lederman, M.M., Offord, R.E., Hartley, O., and Mosier, D.E. (2011) Resistance to the CCR5 inhibitor 5P12-RANTES requires a difficult evolution from CCR5 to CXCR4 coreceptor use. *PLoS One* **6**, e22020
106. Tamamis, P., and Floudas, C.A. (2014) Molecular recognition of CCR5 by an HIV-1 gp120 V3 loop. *PLoS One* **9**, e95767
107. Catasti, P., Fontenot, J.D., Bradbury, E.M., and Gupta, G. (1995) Local and global structural properties of the HIV-MN V3 loop. *J. Biol. Chem.* **270**, 2224–2232
108. Suphaphiphat, P., Essex, M., and Lee, T.-H. (2007) Mutations in the V3 stem versus the V3 crown and C4 region have different effects on the binding and fusion steps of human immunodeficiency virus type 1 gp120 interaction with the CCR5 coreceptor. *Virology* **360**, 182–190
109. Sakaida, H., Hori, T., Yonezawa, A., Sato, A., Isaka, Y., Yoshie, O., Hattori, T., and Uchiyama, T. (1998) T-tropic human immunodeficiency virus type 1 (HIV-1)-derived V3 loop peptides directly bind to CXCR-4 and inhibit T-tropic HIV-1 infection. *J. Virol.* **72**, 9763–9770
110. Salo-Ahen, O.M., Alanko, I., Bhadane, R., Bonvin, A.M., Honorato, R.V., Hossain, S., Juffer, A.H., Kabe-dev, A., Lahtela-Kakkonen, M., Larsen, A.S., Lescrinier, E., Marimuthu, P., Mirza, M.U., Mustafa, G., Nunes-Alves, A., Pansar, T., Saadabadi, A., Singaravelu, K., and Vanmeert, M. (2021) Molecular dynamics simulations in drug discovery and pharmaceutical development. *Processes* **9**, 71
111. Samson, M., LaRosa, G., Libert, F., Paindavoine, P., Detheux, M., Vassart, G., and Parmentier, M. (1997) The second extracellular loop of CCR5 is the major determinant of ligand specificity. *J. Biol. Chem.* **272**, 24934–24941
112. Blanpain, C., Doranz, B.J., Vakili, J., Rucker, J., Govaerts, C., Baik, S.S., Lorthioir, O., Migeotte, I., Libert, F., Baleux, F., Vassart, G., Doms, R.W., and Parmentier, M. (1999) Multiple charged and aromatic residues in CCR5 amino-terminal domain are involved in high affinity binding of both chemokines and HIV-1 Env protein. *J. Biol. Chem.* **274**, 34719–34727
113. Nishikawa, M., Takashima, K., Nishi, T., Furuta, R.A., Kanzaki, N., Yamamoto, Y., and Fujisawa, J.-I. (2005) Analysis of binding sites for the new small-molecule CCR5 antagonist TAK-220 on human CCR5. *Antimicrob. Agents Chemother.* **49**, 4708–4715
114. Dragic, T., Trkola, A., Thompson, D.A., Cormier, E.G., Kajumo, F.A., Maxwell, E., Lin, S.W., Ying, W., Smith, S.O., Sakmar, T.P., and Moore, J.P. (2000) A binding pocket for a small molecule inhibitor of HIV-1 entry within the transmembrane helices of CCR5. *Proc. Natl. Acad. Sci. U. S. A.* **97**, 5639–5644
115. Tsamis, F., Gavrillov, S., Kajumo, F., Seibert, C., Kuhmann, S., Ketas, T., Trkola, A., Palani, A., Clader, J.W., Tagat, J.R., McCombie, S., Baroudy, B., Moore, J.P., Sakmar, T.P., and Dragic, T. (2003) Analysis of the mechanism by which the small-molecule CCR5 antagonists SCH-351125 and SCH-350581 inhibit human immunodeficiency virus type 1 entry. *J. Virol.* **77**, 5201–5208
116. Shaik, M.M., Peng, H., Lu, J., Rits-Volloch, S., Xu, C., Liao, M., and Chen, B. (2019) Structural basis of coreceptor recognition by HIV-1 envelope spike. *Nature* **565**, 318–323
117. Tamamis, P., and Floudas, C.A. (2015) Elucidating a key anti-HIV-1 and cancer-associated axis: the structure of CCL5 (Rantes) in complex with CCR5. *Sci. Rep.* **4**, 1–9
118. Kondru, R., Zhang, J., Ji, C., Mirzadegan, T., Rotstein, D., Sankuratri, S., and Dioszegi, M. (2008) Molecular interactions of CCR5 with major classes of small-molecule anti-HIV CCR5 antagonists. *Mol. Pharmacol.* **73**, 789–800
119. Tan, Y., Tong, P., Wang, J., Zhao, L., Li, J., Yu, Y., Chen, Y.-H., and Wang, J. (2017) The membrane-proximal region of C-C chemokine receptor type 5 participates in the infection of HIV-1. *Front. Immunol.* **8**, 478

120. Recum, H.A.V., and Pokorski, J.K. (2013) Peptide and protein-based inhibitors of HIV-1 co-receptors. *Exp. Biol. Med. (Maywood)* **238**, 442–449
121. Olson, T.S., and Ley, K. (2002) Chemokines and chemokine receptors in leukocyte trafficking. *Am. J. Phys. Regul. Integr. Comp. Phys.* **283**, R7–R28
122. Signoret, N., Pelchen-Matthews, A., Mack, M., Proudfoot, A.E., and Marsh, M. (2000) Endocytosis and recycling of the HIV coreceptor CCR5. *J. Cell Biol* **151**, 1281–1294
123. Jin, T., Xu, X., and Hereld, D. (2008) Chemotaxis, chemokine receptors and human disease. *Cytokine* **44**, 1–8
124. Patterson, B.K., Seethamraju, H., Dhody, K., Corley, M.J., Kazempour, K., Lalezari, J., Pang, A.P., Sugai, C., Mahyari, E., Francisco, E.B., Pise, A., Rodrigues, H., Wu, H.L., Webb, G.M., Park, B.S., Kelly, S., Pourhassan, N., Lelic, A., Kdouh, L., Herrera, M., Hall, E., Bimber, B.N., Plassmeyer, M., Gupta, R., Alpan, O., O'Halloran, J.A., Mudd, P.A., Akalin, E., Ndhlovu, L.C., and Sacha, J.B. (2021) CCR5 inhibition in critical COVID-19 patients decreases inflammatory cytokines, increases CD8 T-cells, and decreases SARS-CoV2 RNA in plasma by day 14. *Int. J. Infect. Dis.* **103**, 25–32